

Thermophysical Study of 1-Butyl-2-Methylpyridinium Tetrafluoroborate Ionic Liquid

Isabel Bandrés,[†] Gorka Pera,[†] Santiago Martín,[†] Miguel Castro,[‡] and Carlos Lafuente^{*,†}

Departamento de Química Orgánica—Química Física, Facultad de Ciencias, Universidad de Zaragoza, 50009 Zaragoza, Spain, and Instituto de Ciencia de Materiales de Aragón, Universidad de Zaragoza-CSIC, 50018 Zaragoza, Spain

Received: June 30, 2009; Revised Manuscript Received: July 14, 2009

A thermophysical study of 1-butyl-2-methylpyridinium tetrafluoroborate in a wide range of temperatures has been performed. Thus, density, speed of sound, refractive index, kinematic viscosity, surface tension, and thermal properties have been measured, whereas coefficients of thermal expansion, molar refractions, dynamic viscosities, and entropies and enthalpies of surface formation per unit surface area at the studied temperatures have been calculated. Experimental results have been compared with those obtained for 1-butyl-3-methylpyridinium tetrafluoroborate and 1-butyl-4-methylpyridinium tetrafluoroborate to analyze the effect of the positional isomeric cationic structure on properties. A systematic characterization leads to understand the behavior of such compounds, being a fundamental step to develop their potential as new solvents.

Introduction

Nowadays, science interest in ionic liquids (ILs) is beyond all doubt, which proves the fact that publication numbers related to these materials in different areas have experienced an exponential growth in the past decade.¹ The unique features of ILs are responsible for the investigation of the field since they provide new options based on different chemical and physical properties, leading to expect useful developments derived from their study. In this way, ILs can offer original solutions to the existing methods and can be the key to the search for new applications in every area of chemistry as their ionic nature gives these materials the potential to behave very differently in contrast to conventional molecular liquids when they are used as solvents. Moreover, by using a IL, it is possible to achieve a broader range of operational temperatures and conditions relative to other conventional media, making them promising chemicals for different purposes.^{2–5}

The lack of knowledge of these novel materials has been discussed as a current barrier to the implementation of ionic liquid technologies, emphasizing real needs for a more fundamental understanding of ionic versus molecular solvents. Specifically, physical and thermodynamic properties have been highlighted as immediate requirements to elucidate any correlation between the chemical structure of the ionic liquids, their ionic interactions, and their properties. This research is essential to evaluate the suitability of these compounds for different applications that make possible their true technological potential.

To solve this matter, our research group is carrying out a systematic study of several pyridinium-based ionic liquids, a less popular family of ILs than those derived from the imidazolium ring that presents interesting properties.^{6–8} Results are analyzed and evaluated, attending to structural and energetic effects in order to achieve a better understanding of these materials.

In this work, we present the thermophysical properties of 1-butyl-2-methylpyridinium tetrafluoroborate ([b2mpy][BF₄]),

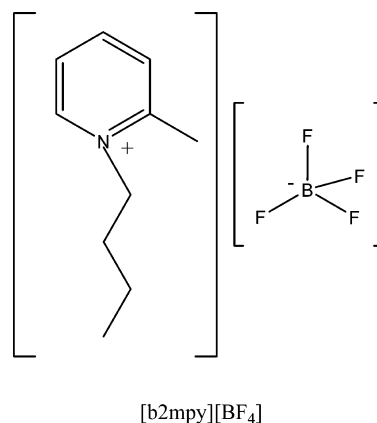


Figure 1. Structure and abbreviation of the ionic liquid under study.

which is shown in Figure 1. Density, speed of sound, refractive index, kinematic viscosity, surface tension, and thermal properties have been measured from 288.15 to 338.15 K. Moreover, coefficients of thermal expansion, molar refractions, dynamic viscosities, and entropies and enthalpies of surface formation per unit surface area at the studied temperatures have been calculated. Densities, dynamic viscosities, and refractive indices at 298.15 and 318.15 K for [b2mpy][BF₄] have been reported before,⁹ and the results fall in the range of our measurements. In order to elucidate the relationship between properties and their molecular features, the results have been compared with those obtained previously for 1-butyl-3-methylpyridinium tetrafluoroborate ([b3mpy][BF₄]), and 1-butyl-4-methylpyridinium tetrafluoroborate ([b4mpy][BF₄]), fluids which share the tetrafluoroborate anion and differ in the methyl group position of the cationic structure. Thus, a comprehensive analysis has been made, paying special attention to the effect of the isomeric cationic structures on the studied properties. To the best of our knowledge, there is not such a study of [b2mpy][BF₄] like the one we present here.

Experimental Section

The ionic liquid 1-butyl-2-methylpyridinium tetrafluoroborate (purity 99%) was provided by IoLiTec. The IL was dried for

* To whom correspondence should be addressed. Phone: +34-976-762295. Fax: +34-976-761202. E-mail: celadi@unizar.es.

[†] Universidad de Zaragoza.

[‡] Universidad de Zaragoza-CSIC.

24 h under a vacuum of ~ 0.05 kPa under stirring and stored before use in a desiccator. Measurements were performed using temperature steps of 2.5 K in the 288.15–338.15 K temperature range.

The densities, ρ , and speeds of sound, u , of the pure compound were determined simultaneously with an Anton Paar DSA 5000 with a temperature control within ± 0.001 K. By measuring the damping of the oscillation of the U-tube caused by the viscosity of the filled-in sample, the DSA 5000 automatically corrects viscosity-related errors in the density. The calibration was carried out with deionized doubly distilled water and dry air. The final uncertainty of the density and speed of sound has been estimated to be $\pm 10^{-5}$ g·cm⁻³ and ± 0.01 m·s⁻¹, respectively.

Refractive indices, n_D , at the 589.3 nm sodium D wavelength were measured using a high-precision automatic refractometer Abbemat-HP DR Kernchen, whose temperature was internally controlled within ± 0.01 K. The apparatus was calibrated with deionized double-distilled water. The corresponding uncertainty is $\pm 1 \times 10^{-6}$.

Surface tensions, σ , were determined using a drop-volume tensiometer Lauda TVT-2.¹⁰ The temperature was kept constant within ± 0.01 K by means of an external Lauda E-200 thermostat. Details of the experimental procedure can be found in a previous paper.¹¹ The uncertainty of the surface tension measurement is ± 0.01 mN·m⁻¹ of the final value of the surface tension.

Kinematic viscosities, ν , were determined using an Ubbelohde viscosimeter with a Schoot–Geräte automatic measuring unit model AVS-440. CaCl₂ drying tubes were used to protect the samples from moisture in the air. The temperature was kept constant within ± 0.01 K by means of a Schoot–Geräte thermostat. The viscosimeter constant was provided by the supplier and was $K = 0.9822$ mm²·s⁻². The uncertainty of the time flow measurements was ± 0.01 s, and the corresponding uncertainty in the kinematic viscosity was ± 0.01 mm²·s⁻¹. From density and kinematic viscosity, the absolute viscosity, η , could be obtained, $\eta = \rho \cdot \nu$, and the estimated uncertainty in the absolute viscosity was ± 0.01 mPa·s.

Two types of calorimetric measurements have been performed in order to characterize the main thermal events. First, isobaric molar heat capacities of the supercooled liquid in the 280–340 K temperature range were determined using a differential scanning calorimeter Q2000 from TA Instruments equipped with a RCS cooling system. Temperature and energy calibrations were made with a standard sample of indium, using its melting transition (429.76 K, 3.296 kJ mol⁻¹). Additionally, in order to determine the heat capacity, the zero-heat-flow procedure described by TA Instruments has been followed using as a standard compound a synthetic sapphire sample measured under the same conditions as the sample (see below). These calibration measurements allow one to estimate an overall uncertainty of ± 0.5 K in temperature and $\pm 3\%$ in the heat capacities. The measurements were carried out using around 8 mg of sample sealed at room temperature in hermetic aluminum pans with a mechanical crimp. Previously, the sample was submitted to a drying vacuum process, and it was exposed to the air only a few minutes during the sealing step. Once inside of the calorimeter and away from room temperature, the liquid sample was cooled down to 278 K, and after equilibration to this temperature, a heating thermogram was performed at a scan rate of 10 K/min up to 343 K.

DSC experiments were also performed in the 100–350 K temperature range, using a differential scanning calorimeter

Q1000 from TA Instruments with the LNCS accessory in order to reach the low-temperature range. In this case, the experiments were performed in a helium gas atmosphere. The measurements were carried out using around 5 mg of sample. Temperature and enthalpy calibrations were also made with standard samples of indium. The procedure for the measurement was the following. First, from room temperature, the sample was cooled down to 100 at 10 K/min, and a subsequent heating up to 340 K at the same scan rate was recorded. Since the sample undergoes upon cooling a crystallization process between 210 and 250 K, we performed another measurement in which a new fresh sample from the liquid state was cooled down to 220 K, maintained for 12 min, and then cooled down to 100 K. This process allowed almost complete crystallization.

The reported glass-transition temperature, T_g , was obtained from the midpoint of the small heat capacity jump upon heating, corresponding to the amorphous glass state, to a liquid-state transformation, whereas the melting temperature was taken to be the onset of an endothermic peak upon heating. For the crystallization, we report the temperature mean value of the corresponding temperature range in which the process happens.

Results and Discussion

A comprehensive set of thermophysical properties is the essential tool to find the relationship between structural characteristics of a novel compound and their features. Each property provides a fraction of information that, studied together as a whole, leads to an understanding of the liquid state that is very useful from the practical and technological points of view. Specifically, the complex nature of ILs allows an investigation of the contribution of both the cationic and the anionic moieties and the different interactions between them in the behavior of these fluids.

In this case, an analysis based on the changes in the substituent position of the pyridinium cation has been carried out by means of the comparison of experimental data for [b2mpy][BF₄], [b3mpy][BF₄], and [b4mpy][BF₄].⁶ This type of investigation is very interesting since it is less usual than others derived from variations in the alkyl chain length of the cation or the anionic nature. It is expected that the knowledge of the correlation between the structure, interactions, and properties of these promising compounds results in the research and the development of new applications related to ILs.

Values of the density, speed of sound, refractive index, molar refraction, surface tension, isobaric molar heat capacity, kinematic viscosity, and dynamic viscosity of the ionic liquid 1-butyl-2-methylpyridinium tetrafluoroborate at the studied temperatures are collected in Table 1. On the other hand, thermal properties are gathered in Table 2.

It should be noted that we have measured the liquid properties in the range of temperatures from 288.15 to 338.15 K, despite the fact that its melting temperature is 301.3 K. Thus, values below 301.3 K are for the supercooled liquid since [b2mpy][BF₄] can remain as a liquid for long periods of time at temperatures well below its melting point.

Thermodynamic properties such as density, refractive index, speed of sound, and surface tension present a linear dependence with temperature in the range of the measurements. Consequently, experimental data for these properties have been correlated, making use of the following equation

$$Y = A \cdot T + B \quad (1)$$

TABLE 1: Experimental Thermophysical Properties of [b2mpy][BF₄] at Atmospheric Pressure as a Function of Temperature

<i>T</i> /K	$\rho/\text{g}\cdot\text{cm}^{-3}$	$\nu/\text{mm}\cdot\text{s}^{-1}$	$\eta/\text{mPa}\cdot\text{s}$	n_D	$R_m/\text{cm}^3\cdot\text{mol}^{-1}$	$\sigma/\text{mN}\cdot\text{m}^{-1}$	$u/\text{m}\cdot\text{s}^{-1}$	$C_{p,m}/\text{J}\cdot\text{mol}^{-1}\cdot\text{K}^{-1}$
288.15	1.20822	711.2	859.3	1.460421	53.778	46.28	1671.42	375
290.65	1.20651	572.7	691.0	1.459729	53.785	46.13	1664.26	376
293.15	1.20478	471.0	567.5	1.459054	53.794	46.02	1657.72	378
295.65	1.20308	389.6	468.7	1.458385	53.802	45.87	1651.13	379
298.15	1.20138	324.1	389.4	1.457715	53.810	45.66	1644.84	380
300.65	1.19967	273.5	328.1	1.457026	53.817	45.54	1638.63	382
303.15	1.19797	230.6	276.3	1.456376	53.827	45.32	1632.50	383
305.65	1.19626	197.4	236.1	1.455696	53.835	45.17	1626.45	384
308.15	1.19460	168.8	201.6	1.455020	53.841	45.08	1620.48	386
310.65	1.19297	145.3	173.3	1.454374	53.848	44.88	1614.57	387
313.15	1.19134	126.2	150.3	1.453705	53.853	44.69	1608.74	388
315.65	1.18970	109.9	130.7	1.453035	53.859	44.54	1602.96	390
318.15	1.18806	96.54	114.7	1.452367	53.864	44.39	1597.21	391
320.65	1.18642	84.93	100.8	1.451722	53.872	44.20	1591.46	392
323.15	1.18478	75.05	88.92	1.451076	53.880	44.06	1585.77	394
325.65	1.18314	66.65	78.86	1.450415	53.886	43.95	1580.10	395
328.15	1.18150	59.52	70.32	1.449751	53.892	43.77	1574.46	396
330.65	1.17986	53.31	62.90	1.449105	53.900	43.68	1568.86	397
333.15	1.17823	47.95	56.50	1.448449	53.906	43.53	1563.24	399
335.65	1.17623	43.32	50.95	1.447817	53.932	43.38	1557.59	401
338.15	1.17499	39.21	46.07	1.447254	53.930	43.21	1552.01	402

TABLE 2: Glass Transition, T_g , Cold Crystallization, T_{cc} , and Melting, T_m , Temperatures for [b2mpy][BF₄] after Cooling the Sample from the Liquid State down to 100 at 10 K·min⁻¹

compound	T_g/K	T_{cc}/K	T_m/K
[b2mpy][BF ₄]	196.5	235	301.3

TABLE 3: Fitting Parameters and Standard Deviations for the Studied Properties for [b2mpy][BF₄]

property	<i>A</i>	<i>B</i>	<i>s</i>
$\rho/\text{g}\cdot\text{cm}^{-3}$	$-6.6510\cdot 10^{-4}$	1.39969	0.00011
n_D	$-2.64563\cdot 10^{-4}$	1.536586	0.000043
$u/\text{m}\cdot\text{s}^{-1}$	-2.36407	2350.04	1.00
$C_{p,m}/\text{J}\cdot\text{mol}^{-1}\cdot\text{K}^{-1}$	0.5356	221	1
$\sigma/\text{mN}\cdot\text{m}^{-1}$	-0.06216	64.20	0.04
	η_0	<i>B</i>	T_0
$\eta/\text{mPa}\cdot\text{s}$	0.106605	935.864	184.077
			<i>s</i>
			1.00

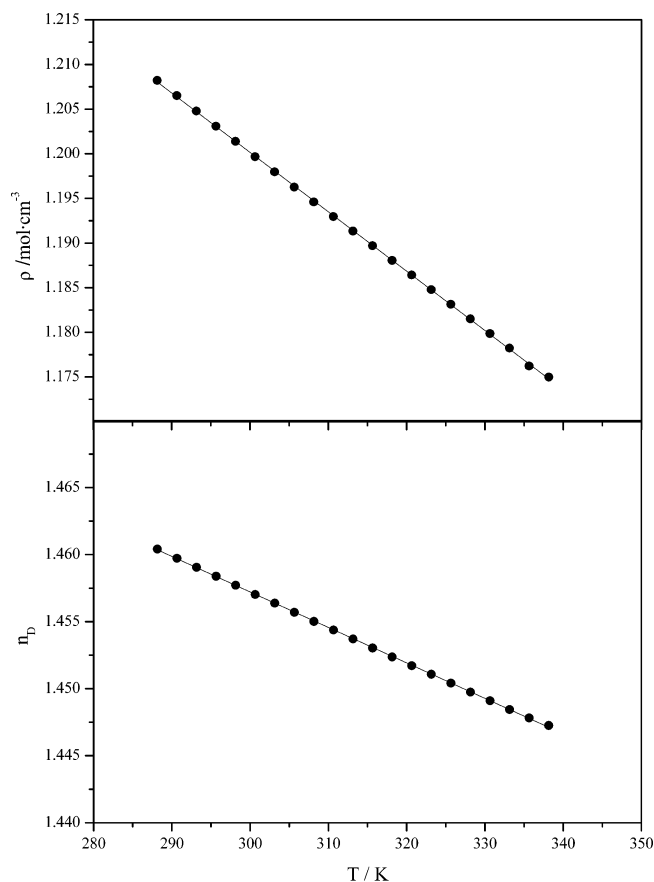
where *Y* is the studied property, *A* and *B* are adjustable parameters, and *T* is the absolute temperature. The best linear fitting parameters and the standard deviations of each property are gathered in Table 3.

Densities of the compound as a function of temperature are shown in Figure 2. As expected, densities decrease linearly with increasing temperature. It is remarkable that values for [b2mpy][BF₄] are greater than those found for the isomers [b3mpy][BF₄] and [b4mpy][BF₄], which are quite similar, and approach the density of the 1-butylpyridinium tetrafluoroborate ([bpy][BF₄])^{12–15} without methylation. That is, the introduction of the alkyl substituent on the pyridinium ring at the C2 position results in high densities. Our density values are slightly lower than those reported by Ortega and co-workers for [b2mpy][BF₄].⁹ Differences are probably related to the application in density values of a correction factor that takes into account the high viscosity of the sample.^{6,16}

The bulk coefficient of thermal expansion, α , can be calculated from the variation of experimental values of density. This coefficient in [b2mpy][BF₄] decreases very slightly when the temperature rises, showing a value of $\alpha = 5.61 \times 10^{-4} \text{ K}^{-1}$ at 298.15 K. Despite the fact that ionic liquid densities are extended in a broad range of values,^{17–20} it has been found that the volumetric expansion of the majority of imidazolium- and

pyridinium-based ionic liquids is in the range of $5\text{--}6 \times 10^{-4} \text{ K}^{-1}$.¹² This suggests that ILs show a similar behavior with temperature. In the same way as high-temperature molten salts, the coefficient is lower than that for most molecular organic liquids.¹²

The dependence of refractive indices on temperature is represented in Figure 2. Experimental data for [b2mpy][BF₄] decrease with a similar slope as their isomeric compounds when the temperature increases, although just as with densities, their

**Figure 2.** Density and refractive index as a function of temperature for [b2mpy][BF₄].

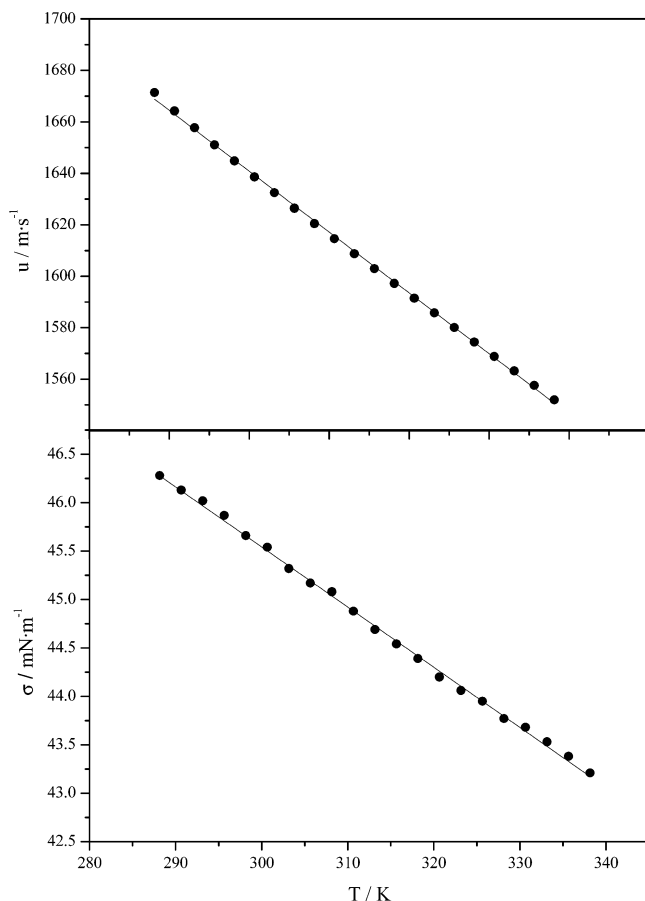


Figure 3. Speed of sound and surface tension as a function of temperature for [b2mpy][BF₄].

values are greater than those for [b3mpy][BF₄] and [b4mpy][BF₄]. Values of the refractive index obtained for [b2mpy][BF₄] at 298.15 and 318.15 K are comparable to those obtained earlier by Ortega et al.⁹ since differences between both data series are less than 0.25%.

The molar refraction, R_m , is a useful property to deepen the understanding of a pure component since it provides an idea of the hard core volume of 1 mole of molecules. Besides, molar refraction and molar volume can be used to obtain by difference the molar free volume, which represents the volume not occupied by ions. Molar refractions have been calculated at the studied temperatures from experimental data of densities and refractive indices using the Lorentz–Lorenz relation, and their values are gathered in Table 1. The comparison with the isomeric ILs indicates that not only the hard core volume but also the free molar volume for [b2mpy][BF₄] is smaller than the values found for [b3mpy][BF₄] and [b4mpy][BF₄]. As we have pointed out before, this volume structure results in a high density for the studied fluid.

The speeds of sound, represented in Figure 3, also decrease in a linear way with temperature. Just as the preceding properties, the values for [b2mpy][BF₄] are greater than the values of the compounds with the methyl group in the C3 and C4 positions.

The temperature dependence of the surface tension is shown in Figure 3. Additionally to the different behavior, it is remarkable the influence of the alkyl substituent position in the ring on the value of the surface tension, being slightly greater for the fluid with the methyl group in the C2 position in the whole range of the measurements.

Previous studies of pure ILs^{21–24} share that this property reflects the effects of both the surface orientation and the intermolecular interactions in the fluid. Therefore, an exhaustive analysis of these factors to facilitate the understanding of the interface is necessary. There are general statements about the microscopic organization of a compound in the surface, such as the Langmuir’s principle of independent surface action, which proclaims that surface tension is a measure of the local free energy of each molecule exposed to the surface.²⁴ To determine the composition and orientation of a compound on the surface, Law et al. have explored the use of direct recoil spectroscopy on several imidazolium-based ionic liquids.²¹ They concluded that both the anion and cation are on the surface. This statement is hardly surprising since the presence of both type of ions to keep a neutral charge on the surface is required. Besides, they suggested that the cation was oriented approximately normal to the surface, and its orientation with respect to the axis of rotation passing through the heterocyclic ring depends on the identity of the alkyl substituent in the cation and the nature of the anion. Considering our work and comparative analysis, our isomeric ILs share the tetrafluoroborate anion and differ from the cationic structure. Therefore, an analysis of results can be made from the substituent position point of view. In this way, we can suggest that the pyridinium ring orients normal to the surface, similar to the imidazolium ring with lower alkyl chain lengths. Thus, the change of the substituent position to C2 might alter the angle of orientation for the cation, with a subsequent increase of the surface tension.

On the other hand, a higher value of this property for [b2mpy][BF₄] is indicative of a stronger intermolecular interaction between the fluid constituents. It is possible that the configuration favors Coulombic or van der Waals interactions not only at the surface but also in the bulk of the ionic liquid. The surface tension results from all of these contributions, being challenging to provide more specific conclusions about the importance of each of them.

From the experimental surface tension measurements, the entropy and enthalpy of surface formation per unit surface area can be evaluated by applying

$$\Delta S = -(\partial\sigma/\partial T)_p \quad (2)$$

$$\Delta H = \sigma - T(\partial\sigma/\partial T)_p \quad (3)$$

Both the entropy and the enthalpy of surface formation per unit area decrease when the temperature increases in the range of the measurements. From experimental data, we have found a value of $\Delta S = 0.06 \text{ mN}\cdot\text{m}^{-1} \text{ K}^{-1}$ and a value of $\Delta H = 64.19 \text{ mN}\cdot\text{m}^{-1}$ for [b2mpy][BF₄] at 298.15 K. Comparing the surface quantities, we notice that both surface parameters for [b2mpy][BF₄] are somewhat smaller than those for [b3mpy][BF₄] and [b4mpy][BF₄].

As it is shown in Figure 4, the temperature dependency of the dynamic viscosity values has been fitted to a Vogel–Fulcher–Tamman equation^{25–27} since it presents convex curved profiles

$$\eta = \eta_0 \exp[B/(T - T_0)] \quad (4)$$

where η_0 , B , and T_0 are the adjustable parameters gathered in Table 3 and T is the absolute temperature. Results indicate that the viscosity of [b2mpy][BF₄] decreases markedly with the

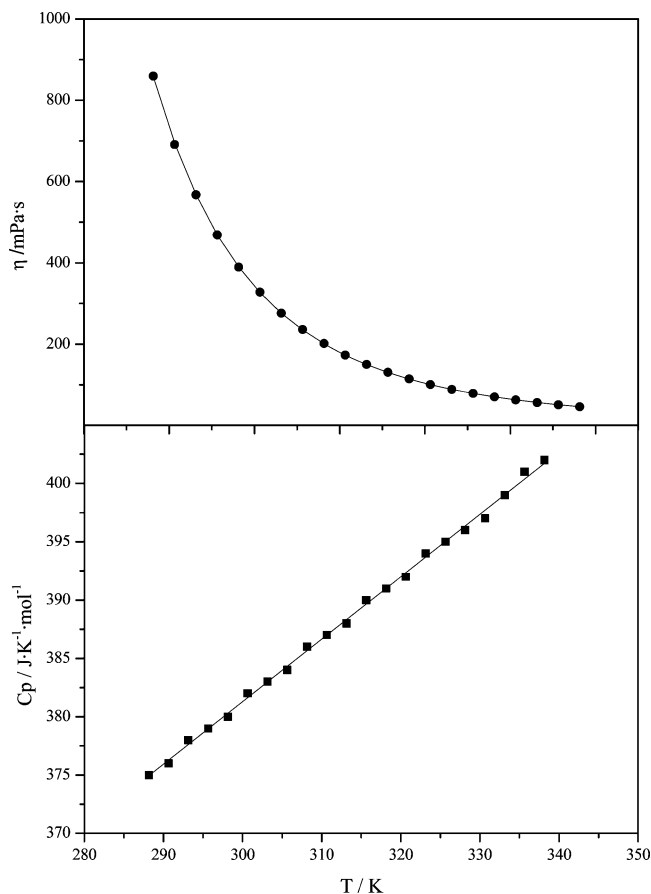


Figure 4. Viscosity and isobaric molar heat capacity as a function of temperature for [b2mpy][BF₄].

increase of temperature. At the light of the experimental values, small changes in the ILs' structure can produce considerable differences in viscosity, the transport property being greater for [b2mpy][BF₄] than that for the isomeric compounds and [bpy][BF₄].^{13,14} The viscosity depends strongly on both the size and shape of the components (ILs with highly symmetric or almost spherical ions are more viscous²⁸) and the intermolecular interactions between them. Thus, a higher viscosity seems to be in agreement with conclusions derived from surface tension data, that is, stronger interactions between the ionic constituents are established in [b2mpy][BF₄]. On the other hand, this larger viscosity can be due in some extent to structural effects as a better accommodation of ions in the fluid, which makes difficult their fluidity. Thus, property values are the result of the combination of all of these factors. Larger differences have been found between our values and those reported before for this property,⁹ probably due to measurements that have been determined by unlike types of viscometers.

Thermal properties of [b2mpy][BF₄] have been investigated by differential scanning calorimetry (see Experimental Section). The isobaric molar heat capacity for the [b2mpy][BF₄] supercooled liquid, shown in Figure 4, increases as the temperature rises. Taking into account the accuracy of the heat capacity measurements, the comparison between these isomeric compounds seems to indicate that the position of the methyl group in the pyridinium cation affects slightly such a property. The heat capacity of the [b2mpy][BF₄] is lower than the values of the [b3mpy][BF₄] and [b4mpy][BF₄] isomers and is near to [bpy][BF₄] values.²⁹ The increase of the number of atoms (increase of the molar mass) and consequently the number of contributing storage modes is behind the larger heat capacity

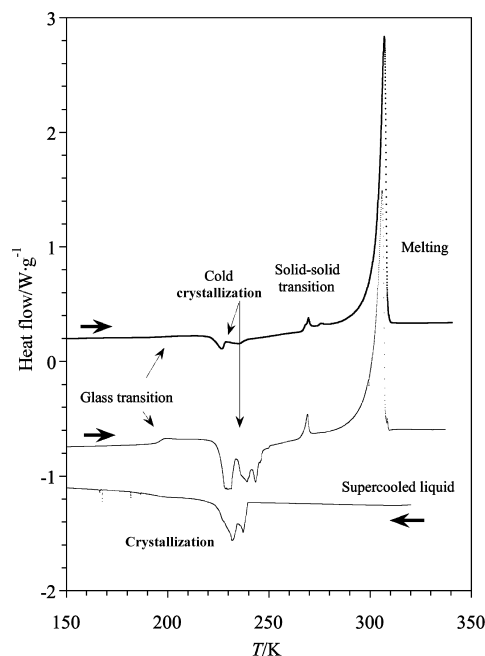


Figure 5. Differential scanning calorimetry results for [b2mpy][BF₄]. The thin line corresponds to the experiment with a cooling process at 10 K/min and the subsequent heating at the same scan rate. The thick line is the heating thermogram after allowing the sample to crystallize at 220 K for 12 min. The latter has been shifted in order to allow the comparison.

of the [b3mpy][BF₄] and [b4mpy][BF₄] with respect to the [bpy][BF₄]. A rough but clear correlation between heat capacity data and the molar mass has been reported by Crosthwaite et al.,³⁰ including a large amount of ionic liquid. However, this dependence cannot explain the lower value of the [b2mpy][BF₄] since it has the same type and number of atoms and molecular groups. The density of the [b2mpy][BF₄] ionic liquid is higher than the [b3mpy][BF₄] and [b4mpy][BF₄] partners, indicating a more efficient packing of the ions when the methyl group is in the C2 position near the N atom and alkyl chain. In this closer arrangement, the more or less free rotational motion of the methyl group at the C3 and C4 positions can be hindered at the C2 position due to larger interactions and steric hindrance decreasing its contribution to the heat capacity and reaching a value close to that of the [bpy][BF₄] ionic liquid. An additional study of the crystal structure will allow one to reveal information which can help to elucidate this aspect.

The complete thermogram corresponding to the cooling at 10 K/min from the liquid phase down to 100 K and heating at the same scan rate up to 340 K is shown in Figure 5. A clear anomaly due to the crystallization process appears at around $T_c \approx 230$ K with an enthalpy content of $\Delta H_c = 4.75 \pm 0.5$ kJ/mol. The methylation at the C2 position favors the crystallization with respect to the C3 and C4 position, which does not allow formation of a crystalline phase at low temperature.⁶ Upon heating, a glass transition is detected at $T_g = 196.5$ K (heat capacity step, $\Delta C_p = 63$ J/mol K), indicating that the crystallization was not complete and therefore the low-temperature solid phase was a mixture of a glass and a crystalline phase. The higher molecular mobility reached from this temperature activates again the crystallization (cold crystallization), which gives a broad anomaly centered at $T_{cc} \approx 235$ K ($\Delta H_{cc} = 8.5 \pm 0.5$ kJ/mol). A small anomaly appears at $T_{ss} = 269$ K and can correspond to a solid–solid phase transition. Recently, a similar anomaly and similar behavior even with several solid–solid

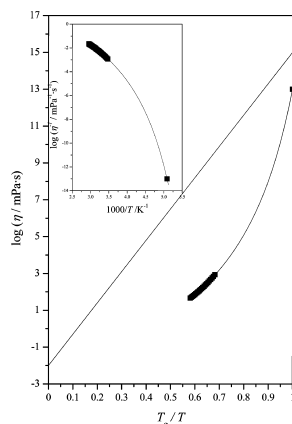


Figure 6. T_g -scaled Arrhenius plot of viscosities of [b2mpy][BF₄]. The inset shows the Arrhenius plot of fluidities of [b2mpy][BF₄] on an expanded scale to include values at the glass-transition temperature.

transitions have been detected in 1-butyl-3-methylimidazolium trifluoroacetate and 1-butyl-3-methylimidazolium nitrate ionic liquids.^{31,32} Finally, a peak corresponding to the melting of the crystalline phase appears at $T_m = 301.3$ K and with $\Delta H_m = 16.5 \pm 0.5$ kJ/mol.

The extent of crystallization upon cooling will depend on the scan rate or on the time spent at a temperature at which the crystallization proceeds. If the sample is allowed to crystallize at 220 K for 12 min, the crystalline fraction reaches almost 100%. The heating thermogram after this process and at 10 K/min from 100 K is also shown in Figure 5. The glass transition is hardly detected at around 196–197 K (with $\Delta C_p \approx 7$ J/mol K), and the anomaly corresponding to the cold crystallization appears at around 240 K with only a small enthalpy content of 2 ± 0.5 kJ/mol. The melting peak appears almost at the same temperature (302.75 K) and with $\Delta H_m = 18.2 \pm 0.5$ kJ/mol, slightly higher than the previous measurement.

Using experimental values of the viscosity and glass-transition temperature, it is possible to classify the compounds between the extremes of the strong and fragile behaviors. These concepts are considered very useful since it has been suggested that they provide an idea about the stability of the short- and medium-range order against temperature-induced degradation.³³ The fragile compounds in general contain nondirectional bonds, molten salts being typical examples of these glass formers. By contrast, strong systems manifest a resistance to structural degradation due to the fact that they often present self-reinforcing tetrahedral network structures.³⁴

Diagrams of the logarithm of the viscosity as a function of (T_g/T) are very helpful in visualizing comparative fragilities. Thus, the representation of a strong compound is hard to distinguish from that of the Arrhenius law, whereas those following the Vogel–Fulcher–Tammann equation are fragile.³⁵ Moreover, this property can be quantified in various ways.³⁵ One of these approaches was proposed by Angell et al.,³³ which used the index $D = B/T_0$ obtained from parameters of the Vogel–Fulcher–Tammann equation as a criterion for classifying compounds. According to Angell, a D value of less than 10 represents a fragile behavior, whereas values are around 100 for strong liquids.³⁴

In Figure 6, the T_g -scaled Arrhenius plot of the viscosity is represented. In the inset, experimental values for fluidities, ϕ , defined as the inverse of the dynamic viscosity of [b2mpy][BF₄] in the common Arrhenius form, are shown. This inset includes the value at its onset point, defined as the glass-transition temperature. The fluidity in this point is the inverse of the

viscosity that has been found for common liquids whose T_g values are below room temperature ($\eta \approx 10^{13}$ mPa·s).

It is noticeable from Figure 6 that [b2mpy][BF₄] shows large deviations from the Arrhenius behavior since viscosity data are situated on the right-hand side of the diagram. It indicates that, in the same way as its isomers, [b2mpy][BF₄] is fragile. Taking into account their situations in the plot, the sequence for the fragility of the considered ILs is [b2mpy][BF₄] > [b3mpy][BF₄] > [b4mpy][BF₄]. Despite the fact that the D parameter proves that these compounds are fragile since their values are lesser than 10, the order attending to this approach is different from that derived from the T_g -scaled Arrhenius plot of the viscosity. Thus, [b2mpy][BF₄] shows a value of $D = 5.08$, which places it in an intermediate position between the others. The slight differences in the behavior of these ILs can explain the discrepancy among the analyzed criteria.

Conclusions

A comprehensive thermophysical characterization of [b2mpy][BF₄] has been performed at a wide range of temperatures. Experimental results for the studied properties have been compared with those obtained previously for both [b3mpy][BF₄] and [b4mpy][BF₄] ionic liquids to evaluate the influence of the methyl group position of the cation on the behavior of ILs. It is highlighted that properties are strongly influenced by changes in the substituents position, finding that experimental values for [b2mpy][BF₄] are greater than those for the isomeric compounds. Only isobaric molar heat capacities are lower for the studied liquid. Moreover, the apparent fragility of [b2mpy][BF₄] has been discussed in structural terms. This research is essential to achieve the needed theoretical understanding about these types of compounds that makes possible the implementation of ionic liquid technologies.

Acknowledgment. We are grateful for financial assistance from Dirección General de Aragón, Universidad de Zaragoza, Spanish Ministerio de Ciencia y Educación (MAT2007-61621 and CSD2007-00010), and the European Union Network of Excellence MAGMANet (NMP3-CT-2005-515767-2). I.B. and G.P. thank the predoctoral fellowship from DGA and MEC, respectively. S.M. acknowledges his Juan de la Cierva contract from MEC.

References and Notes

- (1) Smiglak, M.; Metlen, A.; Rogers, R. D. *Acc. Chem. Res.* **2007**, *40*, 1182.
- (2) Clavel, G.; Larionova, J.; Guari, Y.; Guerin, C. *Chem.—Eur. J.* **2006**, *12*, 3798.
- (3) Rogers, R. D.; Seddon, K. R.; Volkov, S. *Green industrial applications of ionic liquids*; Springer: New York, 2002.
- (4) Koel, M. *Ionic liquids in chemical analysis*; CRC Press: Boca Raton, FL, 2008.
- (5) Wang, Y.; Maksimuk, S.; Shen, R.; Yang, H. *Green Chem.* **2007**, *9*, 1051.
- (6) Bandres, I.; Giner, B.; Artigas, H.; Royo, F. M.; Lafuente, C. *J. Phys. Chem. B* **2008**, *112*, 3077.
- (7) Bandres, I.; Giner, B.; Artigas, H.; Lafuente, C.; Royo, F. M. *J. Chem. Eng. Data* **2009**, *54*, 236.
- (8) Bandres, I.; Giner, B.; Gascon, I.; Castro, M.; Lafuente, C. *J. Phys. Chem. B* **2008**, *112*, 12461.
- (9) Navas, A.; Ortega, J.; Vreekamp, R.; Marrero, E.; Palomar, J. *Ind. Eng. Chem. Res.* **2009**, *48*, 2678.
- (10) Miller, R.; Hofmann, A.; Hartmann, R.; Schano, K. H.; Halbig, A. *Adv. Mater.* **1992**, *4*, 370.
- (11) Giner, B.; Cea, P.; Lopez, M. C.; Royo, M. M.; Lafuente, C. *J. Colloid Interface Sci.* **2004**, *275*, 284.
- (12) Gu, Z. Y.; Brennecke, J. F. *J. Chem. Eng. Data* **2002**, *47*, 339.
- (13) Mokhtarani, B.; Sharifi, A.; Mortaheb, H. R.; Mirzaei, M.; Mafi, M.; Sadeghian, F. *J. Chem. Thermodyn.* **2009**, *41*, 323.

- (14) Noda, A.; Hayamizu, K.; Watanabe, M. *J. Phys. Chem. B* **2001**, *105*, 4603.
- (15) Blanchard, L. A.; Gu, Z. Y.; Brennecke, J. F. *J. Phys. Chem. B* **2001**, *105*, 2437.
- (16) Aparicio, S.; Alcalde, R. *Green Chem.* **2009**, *11*, 65.
- (17) Fredlake, C. P.; Crosthwaite, J. M.; Hert, D. G.; Aki, S.; Brennecke, J. F. *J. Chem. Eng. Data* **2004**, *49*, 954.
- (18) Huddleston, J. G.; Visser, A. E.; Reichert, W. M.; Willauer, H. D.; Broker, G. A.; Rogers, R. D. *Green Chem.* **2001**, *3*, 156.
- (19) Tokuda, H.; Ishii, K.; Susan, M.; Tsuzuki, S.; Hayamizu, K.; Watanabe, M. *J. Phys. Chem. B* **2006**, *110*, 2833.
- (20) Yoshida, Y.; Baba, O.; Larriba, C.; Saito, G. *J. Phys. Chem. B* **2007**, *111*, 12204.
- (21) Law, G.; Watson, P. R. *Chem. Phys. Lett.* **2001**, *345*, 1.
- (22) Freire, M. G.; Carvalho, P. J.; Fernandes, A. M.; Marrucho, I. M.; Queimada, A. J.; Coutinho, J. A. P. *J. Colloid Interface Sci.* **2007**, *314*, 621.
- (23) Law, G.; Watson, P. R. *Langmuir* **2001**, *17*, 6138.
- (24) Kilaru, P.; Baker, G. A.; Scovazzo, P. J. *Chem. Eng. Data* **2007**, *52*, 2306.
- (25) Vogel, H. *Phys. Z.* **1921**, *22*, 645.
- (26) Fulcher, G. S. *J. Am. Ceram. Soc.* **1925**, *8*, 339.
- (27) Tammann, G.; Hesse, W. Z. *Anorg. Allg. Chem.* **1926**, 156.
- (28) Gardas, R. L.; Coutinho, J. A. P. *Fluid Phase Equilib.* **2008**, *266*, 195.
- (29) Zhang, Z. H.; Sun, L. X.; Tan, Z. C.; Xu, F.; Lv, X. C.; Zeng, J. L.; Sawada, Y. *J. Therm. Anal. Calorim.* **2007**, 289.
- (30) Crosthwaite, J. M.; Muldoon, M. J.; Dixon, J. K.; Anderson, J. L.; Brennecke, J. F. *J. Chem. Thermodyn.* **2005**, *37*, 559.
- (31) Strechan, A. A.; Kabo, A. G.; Paulechka, Y. U.; Blokhin, A. V.; Kabo, G. J.; Shaplov, A. S.; Lozinskaya, E. I. *Thermochim. Acta* **2008**, *474*, 25.
- (32) Strechan, A. A.; Paulechka, Y. U.; Blokhin, A. V.; Kabo, G. J. *J. Chem. Thermodyn.* **2008**, *40*, 632.
- (33) Angell, C. A. *J. Non-Cryst. Solids* **1991**, *131*, 13.
- (34) Bohmer, R.; Ngai, K. L.; Angell, C. A.; Plazek, D. J. *J. Chem. Phys.* **1993**, *99*, 4201.
- (35) Anouti, M.; Caillon-Caravanier, M.; Le Floch, C.; Lemordant, D. *J. Phys. Chem. B* **2008**, *112*, 9412.

JP906133T